



Deglacial and Holocene sea–ice variability north of Iceland and response to ocean circulation changes



Xiaotong Xiao^{a,b}, Meixun Zhao^{a,b,*}, Karen Luise Knudsen^c, Longbin Sha^d, Jón Eiríksson^e, Esther Gudmundsdóttir^e, Hui Jiang^f, Zhigang Guo^g

^a Key Laboratory of Marine Chemistry Theory and Technology (Ocean University of China), Ministry of Education/Laboratory of Marine Ecology and Environmental Science, Qingdao National Laboratory for Marine Science and Technology, PR China

^b Institute of Marine Organic Geochemistry, Ocean University of China, 266100 Qingdao, PR China

^c Centre for Past Climate Studies and Arctic Research Centre, Department of Geoscience, Aarhus University, DK-8000 Aarhus C, Denmark

^d Department of Geography & Spatial Information Techniques, Ningbo University, 315211 Ningbo, PR China

^e Science of Institute, University of Iceland, IS-101, Reykjavik, Iceland

^f State Key Laboratory of Estuarine and Coastal Research, East China Normal University, 200062 Shanghai, PR China

^g Department of Environmental Science and Engineering, Fudan University, 220 Handan Road, 200433 Shanghai, PR China

ARTICLE INFO

Article history:

Received 12 November 2016

Received in revised form 3 May 2017

Accepted 7 May 2017

Available online xxxx

Editor: M. Frank

Keywords:

sea ice

IP₂₅

Bølling/Allerød

Younger Dryas

North Icelandic shelf

ABSTRACT

Sea–ice conditions on the North Icelandic shelf constitute a key component for the study of the climatic gradients between the Arctic and the North Atlantic Oceans at the Polar Front between the cold East Icelandic Current delivering Polar surface water and the relatively warm Irminger Current derived from the North Atlantic Current. The variability of sea ice contributes to heat reduction (albedo) and gas exchange between the ocean and the atmosphere, and further affects the deep-water formation. However, lack of long-term and high-resolution sea–ice records in the region hinders the understanding of palaeoceanographic change mechanisms during the last glacial–interglacial cycle. Here, we present a sea–ice record back to 15 ka (cal. ka BP) based on the sea–ice biomarker IP₂₅, phytoplankton biomarker brassicasterol and terrestrial biomarker long-chain *n*-alkanols in piston core MD99-2272 from the North Icelandic shelf. During the Bølling/Allerød (14.7–12.9 ka), the North Icelandic shelf was characterized by extensive spring sea–ice cover linked to reduced flow of warm Atlantic Water and dominant Polar water influence, as well as strong meltwater input in the area. This pattern showed an anti-phase relationship with the ice-free/less ice conditions in marginal areas of the eastern Nordic Seas, where the Atlantic Water inflow was strong, and contributed to an enhanced deep-water formation. Prolonged sea–ice cover with occasional occurrence of seasonal sea ice prevailed during the Younger Dryas (12.9–11.7 ka) interrupted by a brief interval of enhanced Irminger Current and deposition of the Vedde Ash, as opposed to abruptly increased sea–ice conditions in the eastern Nordic Seas. The seasonal sea ice decreased gradually from the Younger Dryas to the onset of the Holocene corresponding to increasing insolation. Ice-free conditions and sea surface warming were observed for the Early Holocene, followed by expansion of sea ice during the Mid-Holocene.

© 2017 Elsevier B.V. All rights reserved.

1. Introduction

Sea–ice cover on the North Icelandic shelf, at the Polar Front separating the North Atlantic and the Arctic Oceans, is principally linked to the advective strength of the relatively warm Irminger Current and the cold East Icelandic Current, which dominate the

* Corresponding author at: Key laboratory of Marine Chemistry Theory and Technology (Ocean University of China), Ministry of Education, 266100 Qingdao, PR China.

E-mail address: maxzhao@ouc.edu.cn (M. Zhao).

surface waters of the region (Fig. 1; Rudels et al., 2005). The Irminger Current is a branch of the North Atlantic Current and its strength is associated with another branch of the North Atlantic Current, the Norwegian Current. The Norwegian Current flows into the eastern Nordic Seas and is linked to the rate of North Atlantic Deep Water (NADW) formation and the strength of the Atlantic Meridional Overturning Circulation (AMOC), substantially influencing the global climate system (cf. Rayner et al., 2011). Furthermore, the waxing and waning of sea–ice extent in the Nordic Seas also significantly influence the NADW formation and AMOC process, as a result of brine formation and freshwater input, respectively (Thornalley et al., 2010).

Previous palaeo-sea-ice reconstructions north of Iceland have mainly been deduced from microfossil, sedimentological and geochemical data, including ice-rafted debris (IRD), stable isotopes, foraminiferal assemblages and diatoms (e.g. Eiríksson et al., 2000; Knudsen et al., 2004; Ślubowska-Woldengen et al., 2008). Poor preservation of foraminifera and diatoms due to carbonate or silica dissolution has limited sea-ice distribution reconstructions in many regions of the Arctic and sub-Arctic (Schlüter and Sauter, 2000; Zamelczyk et al., 2014). A molecular proxy, IP₂₅, mono-unsaturated highly branched isoprenoid (HBI) alkene biosynthesized by sea-ice diatoms (Belt et al., 2007; Brown et al., 2014), has turned out to be well-preserved in Arctic and sub-Arctic marine sediments and has been determined in a sediment core from the central Arctic Ocean during the Miocene, beyond 5.3 Ma (Stein et al., 2016), thus enabling its application for sea-ice assessment even during the distant past. Although there is still a lack of knowledge about the vertical transport, degradation process and environmental controlling factors of this novel biomarker (for details see Belt and Müller, 2013), IP₂₅ has been applied for palaeo-sea-ice reconstructions covering different areas of the Arctic Ocean and sub-Arctic region (cf. Stein et al., 2012; Belt and Müller, 2013 and references therein). However, there is an ambiguous interpretation of the absence of IP₂₅, since the lack of ice cover or, conversely permanent sea-ice cover inhibiting light penetration, can both limit the sea-ice algal growth. Therefore, phytoplankton biomarkers (e.g. brassicasterol or dinosterol), as open water indicators (Volkman, 2003), have been proposed to be used alongside IP₂₅ to distinguish these ambiguous scenarios (Müller et al., 2009). Generally, the lack of both IP₂₅ and phytoplankton biomarker reflects permanent sea-ice cover; the absence of IP₂₅ with elevated phytoplankton biomarker indicates an open-water condition; while the occurrence of both biomarkers suggests stable sea-ice margin or seasonal sea-ice condition (Müller et al., 2009). Furthermore, the new PIP₂₅ (Phytoplankton-IP₂₅) index, a combination of IP₂₅ and phytoplankton biomarker, was initially developed (Müller et al., 2011) to reconstruct the intensity of spring and summer sea-ice cover semi-quantitatively. By combining new data from high-Arctic realm surface sediments with published data from Arctic marginal areas, Xiao et al. (2015) found a pronounced correlation between PIP₂₅ index values and satellite sea-ice concentrations, providing strong support for a broad application of the PIP₂₅ index.

IP₂₅-based sea-ice reconstructions have been conducted for sediment cores from the Icelandic shelf. IP₂₅ was below detection limit in a sediment core from the southwest of Iceland (Axford et al., 2011) as sea ice did not reach this area over the past 2000 yr, while Andrews et al. (2009) reconstructed the sea-ice condition in a low-resolution sampling core on the Northwest Icelandic shelf during the past 2000 yr by means of multiple proxies including IP₂₅. High-resolution IP₂₅ records, established by Massé et al. (2008) and Cabedo-Sanz et al. (2016) in sediment cores from the North Icelandic shelf, revealed significant sea-ice variability during the past 1200 yr and 8000 yr, respectively. High-resolution IP₂₅ records beyond the Holocene from the Icelandic shelf, however, are required to further understand rapid sea-ice variations and their responses to oceanic changes in detail.

Here, we present high-resolution (20 and 26 yr) biomarker records in marine sediment core MD99-2272 from the North Icelandic shelf during the last deglaciation and relatively lower-resolution (mostly about 100 yr) records during the Early to Mid-Holocene to assess the sea-ice conditions under different oceanic environments. Core site MD99-2272 (Fig. 1) is located in the frontal area between the Irminger Current and the East Icelandic Current, close to fjords influenced by glacial rivers from the Vatnajökull ice cap in Iceland, ideally archiving changes in the oceanic circulation system of the North Atlantic. To evaluate

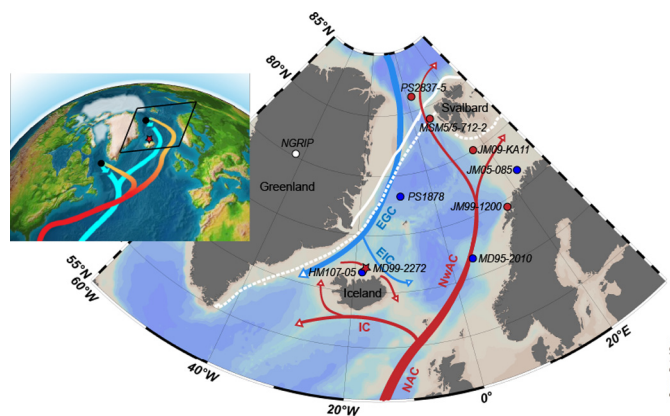


Fig. 1. Study area with the MD99-2272 core location (red star) used for our IP₂₅ study on the North Icelandic shelf. Black dots in the left-hand map represent two areas of deep-water formation in the North Atlantic, and the black rhombus shows the extent of the Nordic Seas (modified from <http://en.es-static.us>). The modern average summer sea-ice extent (white line) and winter sea-ice extent (white dotted line) are indicated in the right-hand map. Red arrows show the surface circulation of warm Atlantic Water entering the Nordic Seas (NAC = North Atlantic Current, NwAC = Norwegian Atlantic Current, IC = Irminger Current), while blue arrows show the circulation patterns of the cold Polar water (EGC = East Greenland Current, EIC = East Icelandic Current). Red dots and blue dots refer to the core sites for IP₂₅ records (Fig. 4) and isotope records (Fig. 5), respectively. White dot on Greenland is the location of the NGRIP ice core. The right-hand map was generated using Ocean Data View (Schlitzer, 2017). (For interpretation of the references to color in this figure legend, the reader is referred to the web version of this article.)

the sea-ice changes and related sea surface conditions, we compare an IP₂₅ record with the phytoplankton biomarker brassicasterol record (an open-water indicator) and the terrestrial biomarker long-chain *n*-alkanols record (a freshwater input indicator; derived from leaf waxes of land plants, Englin-ton and Englin-ton, 2008) from MD99-2272. We also compare the IP₂₅ record of MD99-2272 with the same proxy records in sediment cores from the Fram Strait and eastern Nordic Seas to assess oceanographic processes at a larger scale of the northern North Atlantic during the critical period of the last deglaciation. In addition, we focus on high-resolution sea-ice variability during the last deglaciation and its linkage with insolation, current circulation and AMOC changes, which influence this critical region for the global thermohaline circulation.

2. Regional setting

Iceland is located in the northern North Atlantic (Fig. 1), an area which is sensitive to climate changes. Atmosphere-ocean interactions during abrupt climate shifts are therefore detectable in marine sediment cores from the area (cf. Jiang et al., 2015). Modeling experiments have shown that Iceland was extremely sensitive and vulnerable to temperature change, with just 3 °C of cooling being sufficient to create an ice sheet covering half the present land area (Hubbard et al., 2006). Today, the hydrography of this area is dominated by the cold East Greenland Current and East Icelandic Current from the Arctic Ocean, and the relatively warm and saline Irminger Current, a branch of the North Atlantic Current (Fig. 1; Rudels et al., 2005) which flows along the southern, western and northern shelf of Iceland. Furthermore, the northward flowing warm Atlantic Water becomes cold and dense in the Nordic Seas, northeast of Iceland. Here, cooled Atlantic Water sinks and forms the NADW which overflows the Iceland-Faeroe ridge towards south, associated with the AMOC (Fig. 1; Rayner et al., 2011).

At present, glaciers and ice caps cover ca. 10% of Iceland's area, locking up a considerable volume of freshwater (Ingólfsson et al., 2016), while during the glacial, Iceland and the surrounding

Table 1
Age-depth model boundaries for core MD99-2272 and sedimentation rates.

| Top depth (cm) | Base depth (cm) | Base age (cal. yr BP) | Sedimentation rate (cm/kyr) | Base boundary, Tephra maker |
|----------------|-----------------|-----------------------|-----------------------------|-----------------------------|
| 0 | 14 | 233 | 62 | V1717 |
| 14 | 46.5 | 473 | 135 | V1477 |
| 46.5 | 253.5 | 2980 | 82 | Hekla 3 |
| 253.5 | 355.5 | 4200 | 84 | Hekla 4 |
| 355.5 | 487.5 | 6650 | 54 | Hekla -DH |
| 487.5 | 527.5 | 7050 | 100 | Hekla 5 |
| 527.5 | 776.5 | 10300 | 77 | Saksunarvatn ash |
| 776.5 | 1221.5 | 12120 | 244 | Vedde Ash |
| 1221.5 | 1696.5 | 14550 | 195 | Borrobol |

shallow shelf were nearly fully covered by the Iceland Ice Sheet (Hubbard et al., 2006). The advance and retreat of the Iceland Ice Sheet, as well as isostatic adjustments were of substantial importance to North Atlantic sea level changes, response to the climate forcing (i.e., solar insolation) and oceanic variability (i.e., circulation and deep-water formation) (Norðdahl and Ingólfsson, 2015).

It is well known that Iceland is characterized by active volcanic processes which could change ice volume and induce rapid collapses of the ice sheet, resulting in large pulses of meltwater or ice-bergs into the North Atlantic. The volcanism also produced tephra, potentially deposited on the sea floor and imbedded in the sediment record as important chronological markers (Eiríksson et al., 2000; Knudsen and Eiríksson, 2002; Knudsen et al., 2004).

3. Materials and methods

3.1. Sediment core and chronology

Piston core MD99-2272 (66°59'34"N; 17°58'29"W, 410 m water depth) was recovered from the North Icelandic shelf (Fig. 1) during the RV *Marion Dufresne* Expedition MD114 in 1999, with a total length of 22.60 m. The interval at 3.40–17.80 m in the sediment core was sampled at every 10 cm between 3.40 and 7.70 m, every 15 cm at 7.70–9.05 m and every 5 cm at 9.05–17.80 m for biomarker analysis, covering the time interval of 15.0–4.0 ka, which represents the younger part of the last deglaciation and Early to Mid-Holocene.

The chronology of core MD99-2272, which was initially published by Knudsen and Eiríksson (2002), has been updated based on tephra markers rather than AMS ¹⁴C dates. The age model for this study was constructed using nine tephra markers as age zone boundaries (Table 1) and an estimated top core age of zero (AD 1950). Major element geochemical analyses of samples from core MD99-2272 have been used to correlate tephra markers with markers in neighbouring cores (Gudmundsdóttir et al., 2012). The identified tephra markers are shown in Table 1 (Knudsen and Eiríksson, 2002; Larsen et al., 2002; Rasmussen et al., 2006; Gudmundsdóttir et al., 2012). The core chronology builds on a linear interpolation between calibrated ages (Fig. 2). The sedimentation rate for the interval between 1221.5 and 1696.5 cm is extrapolated and used for all data points below 1696.5 cm in the core. All ages are given in calibrated years before present (AD 1950).

3.2. Biomarker analysis

The IP₂₅ extraction and purification follow the procedure of Müller et al. (2011), and the sterol and *n*-alkanols extraction and purification follow the procedure of Zhao et al. (2006). Briefly, about 5–8 g sediment samples were freeze-dried and homogenized before any further treatment. Prior to the biomarker analyses, the internal standards 7-hexylnonadecane and C₁₉ *n*-alkanol were added to the sediments for quantification. Subsequently, the

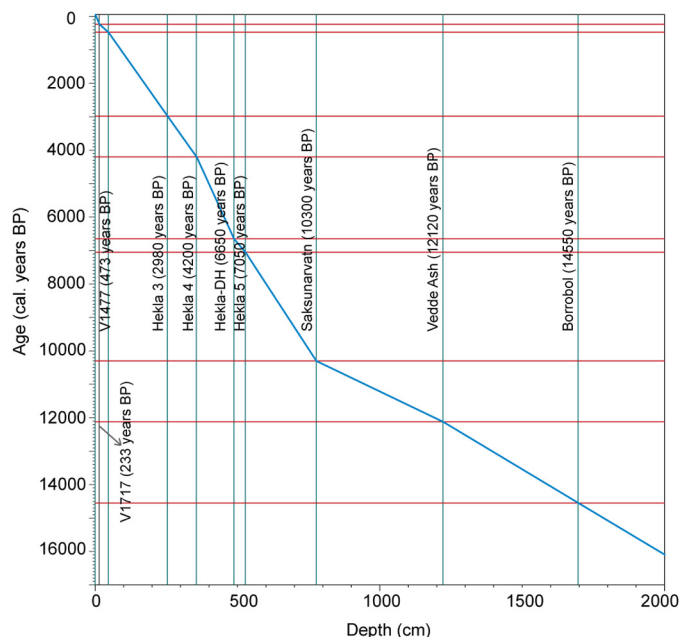


Fig. 2. Calibrated age-depth model for core MD99-2272. The positions of the identified tephra used as age boundaries are marked with green vertical and red horizontal lines, respectively. (For interpretation of the references to color in this figure legend, the reader is referred to the web version of this article.)

sediments were solvent extracted ultrasonically four times using dichloromethane:methanol (2:1 v/v) as solvent. Further separation of hydrocarbons (containing IP₂₅) and alcohols (containing sterols and *n*-alkanols) was carried out via open-column chromatography using SiO₂ as a stationary phase using 8 ml *n*-hexane and 12 ml dichloromethane:methanol (95:5 v/v), respectively. Alcohols were silylated with 40 µl BSTFA (bis-trimethylsilyl-trifluoroacetamide; 70 °C, 1 h) after elution. IP₂₅ was analyzed by gas chromatography (Agilent 7890A GC; 30 m HP-5MS column, 0.25 mm i.d., 0.25 µm film thickness) coupled to an Agilent 5975 C VL mass selective detector (MSD, 70 eV constant ionization potential, ion source temperature 230 °C). The oven was kept initially at 60 °C for 3 min and then programmed to 150 °C at 15 °C/min, followed by 10 °C/min to 320 °C holding for 15 min. Sterols and *n*-alkanols were analyzed by gas chromatography (Agilent 6890N GC; 30 m HP-1 capillary column, 0.32 mm i.d., 0.17 µm film thickness). The oven was kept initially at 80 °C for 1 min and then programmed to 200 °C at 25 °C/min, followed by 4 °C/min to 250 °C, 1.7 °C/min to 300 °C for 10 min, and finally 310 °C holding for 8 min. For the quantification of IP₂₅ its molecular ion (m/z 350) in relation to the ion of internal standard 7-hexylnonadecane (m/z 266) was used. The content of sterols and *n*-alkanols were calculated from the ratio of their GC peak integrations to that of the C₁₉ *n*-alkanol IS. The biomarker concentrations are reported as ng/g of bulk dry weight sediment.

3.3. Calculation of PIP₂₅

The phytoplankton-IP₂₅ (PIP₂₅) index was defined by Müller et al. (2011):

$$PIP_{25} = IP_{25} / (IP_{25} + \text{phytoplankton} \cdot c)$$

with *c* = mean IP₂₅ concentration/mean phytoplankton concentration.

Since IP₂₅ is a trace compound and only detectable by GC-MS selected ion monitoring in most cases, the *c*-factor is proposed to compensate the significant imbalance caused by the different orders of magnitude between low IP₂₅ concentration and high phyto-

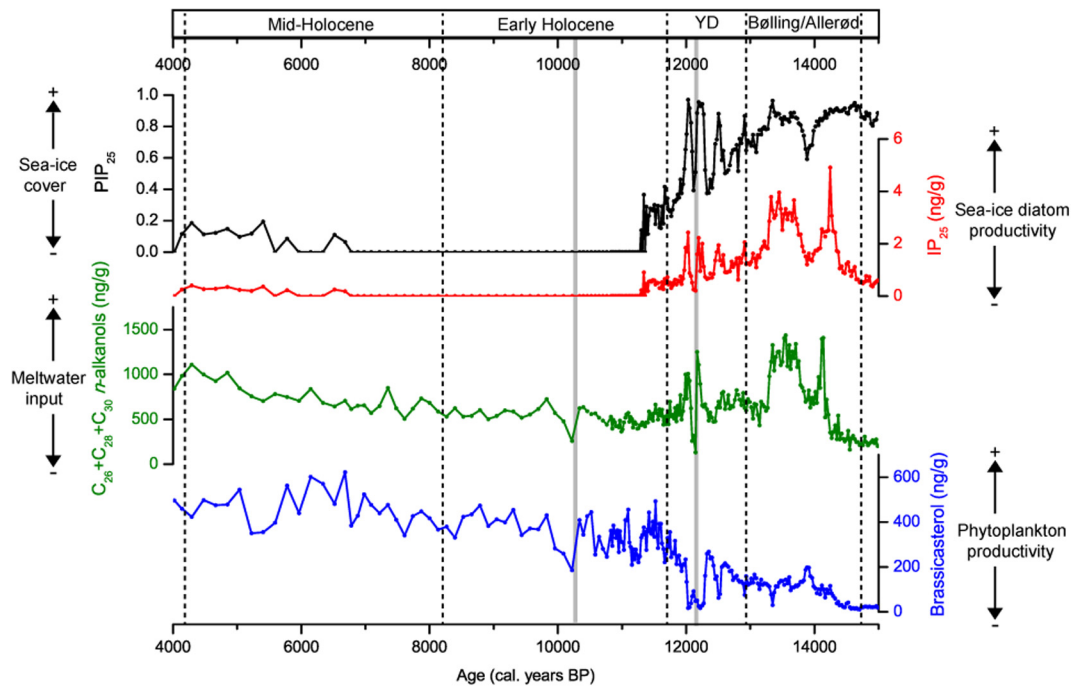


Fig. 3. Biomarker concentrations and PIP_{25} index in core MD99-2272. Light gray bars indicate the Saksunarvatn ash (10.3 ka) and Vedde Ash (12.1 ka), respectively. (For interpretation of the references to color in this figure legend, the reader is referred to the web version of this article.)

plankton biomarker concentration. Despite the limitations and difficulties arising from the employment of this balance factor (c) (for details see Belt and Müller, 2013), the PIP_{25} index has been widely applied in both surface and core sediments. Brassicasterol-based PIP_{25} (P_BIP_{25}) values showed a better correlation with sea-ice concentrations both in the original study from the Fram Strait (Müller et al., 2011) and in the overview study with a comprehensive data set across the Arctic (Xiao et al., 2015) than other phytoplankton biomarkers (e.g., dinosterol and short chain n -alkanes). Thus, we also use brassicasterol as the phytoplankton biomarker to calculate the PIP_{25} (P_BIP_{25}) values in this study. Recently, a HBI triene has been used as a phytoplankton biomarker together with IP_{25} to calculate PIP_{25} (the so called $P_{III}IP_{25}$), because the magnitude of triene concentrations is comparable to that of IP_{25} concentrations that can avoid the uncertainty of balance factor (c) (Belt et al., 2015; Smik et al., 2016).

4. Results

A total of 228 samples from MD99-2272 was analyzed for IP_{25} , sterol and n -alkanol contents. IP_{25} contents are in the range of 0–4.9 ng/g (ng/g of bulk dry weight sediment) with an average value of 1.1 ng/g (Fig. 3). The Bølling/Allerød (14.7–12.9 ka) interval was characterized by generally high concentrations of IP_{25} , with the highest concentration (4.9 ng/g) at 14.3 ka. A lower IP_{25} concentration (1.2 ng/g) is detected in sediments between the Bølling and Allerød intervals at 13.9 ka. During the Younger Dryas (12.9–11.7 ka), IP_{25} values show strong variability between 0.2 ng/g and 2.4 ng/g in sediments. IP_{25} drops to zero values in sediments at 11.3 ka during the Early Holocene until 6.8 ka. Subsequently, IP_{25} shows generally low values (0–0.4 ng/g) in sediments until 4 ka.

Brassicasterol values (Fig. 3) are generally low (10–355 ng/g) in sediments during the Bølling/Allerød and Younger Dryas periods, and reach minimum values (17–92 ng/g) in sediments between 12.3 and 12.2 ka during the Younger Dryas. A generally positive trend is observed for brassicasterol concentrations during the Early

and Mid-Holocene (11.7–4 ka) with obvious and strong fluctuations, reaching the highest values at 7–6 ka.

In general, P_BIP_{25} values are high (0.64–0.97) during the Bølling/Allerød and are strongly variable (0.14–0.98) during the Younger Dryas (Fig. 3). Zero values of P_BIP_{25} occur during the Early Holocene and part of the Mid-Holocene, but P_BIP_{25} gradually increase after ca. 6.8 ka maintaining low values (<0.23) until ca. 4 ka.

The contents of long-chain $C_{26} + C_{28} + C_{30}$ n -alkanols range from 131 to 1404 ng/g (Fig. 3). The highest value (1404 ng/g) is detected in sediments at 13.5 ka during the Bølling/Allerød, while the concentrations decrease during the transition from the Bølling/Allerød to the Younger Dryas. There is an abrupt decrease to the lowest value (131 ng/g) at ca. 12.2 ka in the Vedde tephra layer during the Younger Dryas interval. We observe gradually increased long-chain n -alkanols concentrations (260–1220 ng/g) in sediments during Early and Mid-Holocene, with a distinct decrease at ca. 10.3 ka.

The HBI triene concentrations are in the range of 0–3.48 ng/g, with general low values in sediments during Bølling/Allerød and Younger Dryas and abrupt increased values during the Early Holocene (Fig. A1). $P_{III}IP_{25}$ values strongly vary (0.21–1.0) in sediments during the Bølling/Allerød and the Younger Dryas, and show zero values during the Early Holocene and part of the Mid-Holocene (Fig. A1).

5. Discussion

The data presented in this study allow us to reconstruct the sea-ice conditions on the North Icelandic shelf during the last deglaciation and in the Early and Mid-Holocene. Sea-ice variability in the area was controlled by several factors, e.g., alternations of the palaeocirculation, the freshwater input due to ice sheet melting, as well as changes in insolation and atmospheric forcing. Previous studies reported that the northern North Atlantic was influenced by drift-ice export through the Fram Strait from the Arctic Ocean during the Younger Dryas and Holocene (Not and Hillaire-Marcel, 2012; Cabedo-Sanz et al., 2016). How-

ever, Knudsen et al. (2004) concluded that isotope values and variability in planktonic and benthic foraminifera indicated brine formation caused by local freezing of surface waters at the same location as core site MD99-2272 during the early part of the Bølling-Allerød complex and during the Younger Dryas. Dokken and Jansen (1999) also pointed out that shelf areas (including the coast of Iceland) were potential source areas for intensive sea-ice formation. These studies indicate that the sea ice on the North Icelandic shelf was presumably mainly formed in situ during the last deglaciation, but that the influence of the allochthonous drift ice cannot be ignored. Thus, we interpret the IP₂₅ biomarker as an indicator of in-situ formed sea ice in the area. In addition, we observe similar trends of IP₂₅ and long-chain *n*-alkanols of core MD99-2272 during the Bølling/Allerød and Younger Dryas (Fig. 3). Continuous wavelet analyses show quite similar periodic patterns of IP₂₅ and long-chain *n*-alkanols (Fig. A2a and b), and wavelet coherence analyses reveal that IP₂₅ and long-chain *n*-alkanols display clear coherency (Fig. A2c). Therefore, it is probable that freshwater input has substantially influenced the sea-ice formation on the North Icelandic shelf during the Bølling/Allerød and Younger Dryas. Furthermore, considering the possible influence of allochthonous drift ice from the Arctic Ocean and the lack of surface sediment-based calibration of the PIP₂₅ in the study area, the interpretation of P_BIP₂₅ has been restricted. The variability patterns of P_BIP₂₅ (brassicasterol based PIP₂₅) and P_{III}IP₂₅ (triene based PIP₂₅) are broadly similar in our study (Fig. A1). We use P_BIP₂₅ to interpret sea-ice conditions rather than P_{III}IP₂₅ for the North Icelandic shelf because the producer of triene is yet unidentified, and it is totally absent in the ice-free scenario on the West Icelandic shelf (Cabedo-Sanz et al., 2016). Thus, there is still an uncertainty associated with using triene as an open water indicator, at least on the Icelandic shelf.

Based on biomarker changes, the records have been subdivided into three time intervals for discussion, i.e. the Bølling/Allerød (14.7–12.9 ka), the Younger Dryas (12.9–11.7 ka) and the Early to Mid-Holocene (11.7–4.0 ka). The IP₂₅ record of Bølling/Allerød and Younger Dryas intervals are compared with the same proxy records in sediment cores from different areas (Fig. 4).

5.1. Extensive sea-ice cover during the Bølling/Allerød (14.7–12.9 ka)

An extensive spring/summer sea-ice cover at the core site during the initial interval (ca. 14.7–13.9 ka) of the Bølling/Allerød is indicated by a significant increase of IP₂₅ concentration to the highest values, and low brassicasterol concentrations (Fig. 3). This is also supported by the high values of the P_BIP₂₅ index (average 0.86; Fig. 3). Ocean circulation changes presumably played an important part in the sea-ice expansion during this interval. The cold East Icelandic Current probably dominated the study area, considering that a diatom study of the neighboring core HM107-05 (Fig. 1) revealed that the *T. Antarctica* resting spores became the most important component of the diatom assemblage during the interval 15–13.8 ka (Knudsen et al., 2004). Apparently, the Irminger Current ceased at the same time, and cold bottom waters entered the area, as indicated by the dominance of high-arctic benthic foraminiferal species and the almost disappearance of planktonic foraminifera (Eiriksson et al., 2000). The combination of East Icelandic Current domination and Irminger Current reduction resulted in surface water freezing in the area, triggering sea-ice expansion. In addition, high concentrations of long-chain *n*-alkanols (Fig. 3) provide evidence of a large volume of freshwater input to the cold sea surface area of the North Icelandic shelf, consistent with a decrease in planktonic foraminifera and planktonic foraminiferal $\delta^{18}\text{O}$ at the same location as core site MD99-2272 (Fig. 5; Eiriksson et al., 2000; Knudsen et al., 2004). This was taken to indicate brine formation caused by local freez-

ing of surface waters, i.e. sea-ice formation. The freshwater input to the core site was mainly caused by meltwater pulse 1A (MWP-1A) deriving from the collapse of the Greenland and Iceland ice sheets at 14.5 ka (cf. Telesinski et al., 2014a, 2014b; Norðdahl and Ingólfsson, 2015), which caused high accumulation of terrestrial organic matter.

A similar mechanism can also be applied to interpret sea-ice conditions during the later part (ca. 13.9–12.9 ka) of the Bølling/Allerød. Substantial sea-ice cover is indicated by high IP₂₅ and low brassicasterol and HBI triene concentrations, as well as high values of P_BIP₂₅ index (Fig. 3). The strong influence of Polar water via the East Icelandic Current and a ceased Irminger Current resulted in an increase in sea-ice coverage (Eiriksson et al., 2000; Knudsen et al., 2004). However, a short period (ca. 14.0–13.8 ka) of distinctly reduced IP₂₅ concentrations together with a synchronous decrease in NGRIP $\delta^{18}\text{O}$ was observed within the Bølling/Allerød (Figs. 3 and 5). This was caused by abrupt cooling rather than by a circulation change. This cold period, the Older Dryas (cf. Knies, 2005), is reflected by a re-advance of the ice sheet and further increase of sea-ice thickness which reduced the light penetration thus inhibiting the ice algae growth. In addition, the increase in sea ice over the core site hindered the input of terrestrial material via freshwater, as revealed by reduced long-chain *n*-alkanol concentrations (Fig. 3). The decreased IP₂₅ concentrations and continued low brassicasterol concentrations, however, resulted in reduced PIP₂₅ values during this short cold period (Fig. 3). Thus, careful evaluation of individual biomarker concentrations is required to avoid misleading interpretation when using PIP₂₅ to estimate the sea-ice conditions (for details see Müller et al., 2011).

Generally, our results indicate that North Icelandic shelf conditions during the Bølling/Allerød were harsh with pronounced sea-ice cover and decreased influence of Atlantic Water (Eiriksson et al., 2000; Knudsen et al., 2004; Ślubowska-Woldengen et al., 2008). This provided suitable living conditions for ice algae but inhibited phytoplankton growth, thus yielding high IP₂₅ concentrations but low brassicasterol concentrations in the underlying sediments. Similar environmental conditions were also reconstructed in sediment cores further north of the Iceland from the Fram Strait at high latitudes (79–81°N) (Yermak Plateau and west of Svalbard, Fig. 1). In that area elevated IP₂₅ concentrations and high PIP₂₅ values are observed in the sediments during the Bølling/Allerød (Figs. 4 and A3), as a result of the influence of meltwater from the Svalbard-Barents Sea Ice Sheet (Müller et al., 2009; Müller and Stein, 2014). Müller and Stein (2014) also reported high concentrations of terrestrial, potentially meltwater-derived organic matter from the western continental margin of Svalbard. In contrast, the IP₂₅ and PIP₂₅ values obtained from sediment cores from the eastern Nordic Seas (western Barents Sea and northwest of Norway; Fig. 1) showed low and/or zero values (Figs. 4 and A3), at least during the Allerød period, indicating less-ice or ice-free conditions (Cabedo-Sanz et al., 2013; Belt et al., 2015). Altogether, our new results and previous results suggest anti-phase sea-ice conditions between the western and eastern Nordic Seas in the sub-Arctic region.

5.2. Fluctuations of sea-ice cover during the Younger Dryas (12.9–11.7 ka)

The Younger Dryas event was a period of rapid cooling in the Northern Hemisphere, driven by atmospheric and oceanic circulation changes (Bakke et al., 2009), resulting in low NGRIP $\delta^{18}\text{O}$ values (Fig. 5). Generally, the cooling resulted in intermediate IP₂₅ concentrations and low brassicasterol during the Younger Dryas (Fig. 3), as the harsh conditions favored sea-ice formation and hampered marine productivity. Both IP₂₅ and PIP₂₅ values show strong variability during the Younger Dryas (Fig. 3), indicating

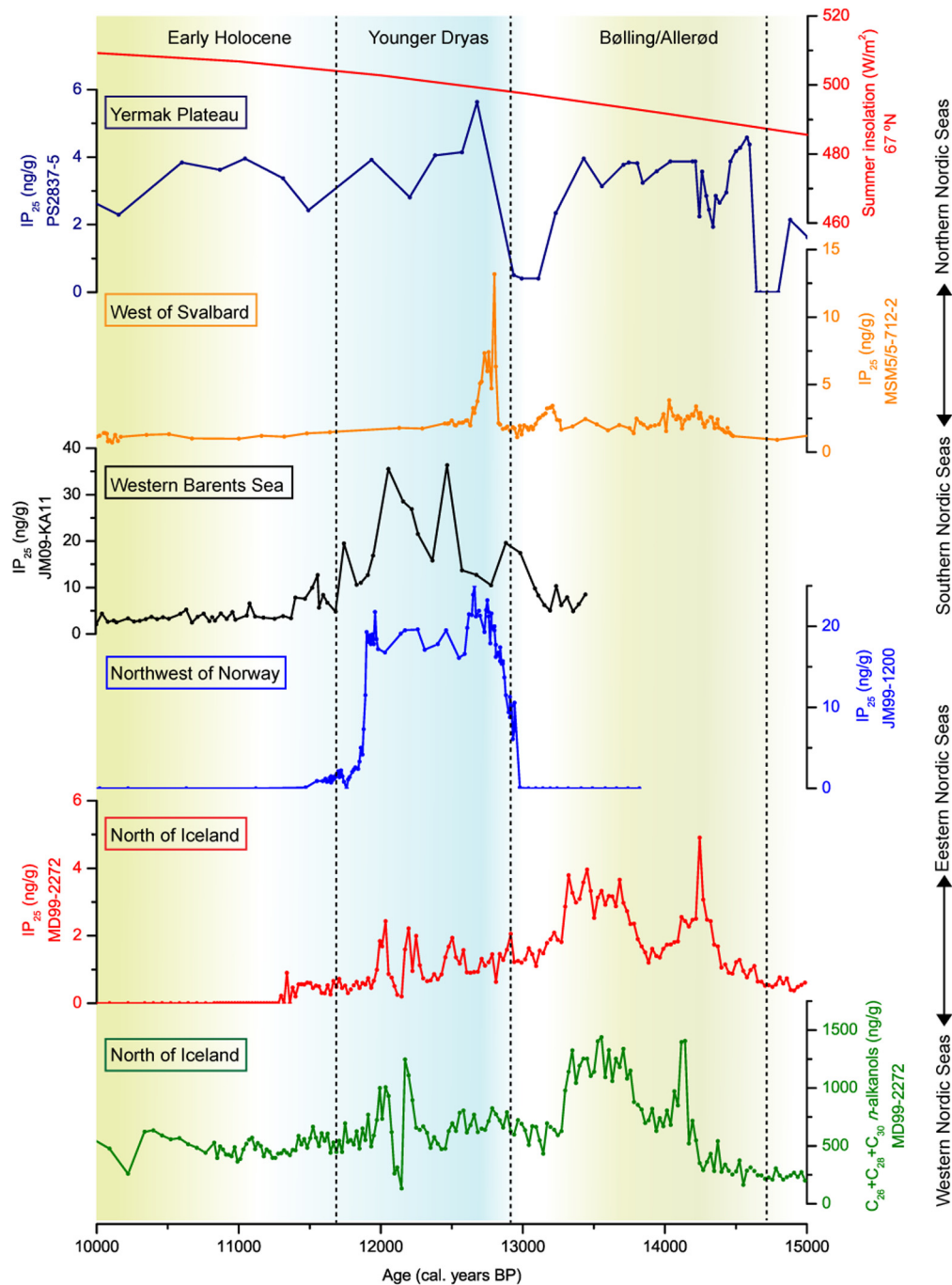


Fig. 4. Compilation of sea-ice proxy records for various regions with the terrestrial record on the North Icelandic shelf: IP₂₅ concentrations in PS2837-5 (Müller et al., 2009); IP₂₅ concentrations in MSM5/5-723-2 (Müller and Stein, 2014); IP₂₅ concentrations in JM09-KA11 (Belt et al., 2015); IP₂₅ concentrations in JM99-1200 (Cabedo-Sanz et al., 2016); IP₂₅ concentrations in MD99-2272 (this study); long-chain *n*-alkanols concentrations in MD99-2272 (this study).

strong fluctuations in sea ice between seasonal sea-ice cover and permanent sea-ice condition on the North Icelandic shelf. Similarly, the increase of pebble content (interpreted as IRD) in neighboring core HM107-05, contributed by ice-bergs from calving valley glaciers, as well as material released by coastal ice floes breaking away from the sea shores of Iceland (Knudsen et al., 2004), indicate the occurrence of sea ice in the study area. Also, these studies show fluctuations in the flux of planktonic foraminifera due to changes in sea-ice cover, supporting the biomarker records. High abundances of *Cassidulina neoteretis* (subarctic foraminiferal species related to Atlantic Water) indicate that the warm Atlantic Water via the Irminger Current penetrated to the subsurface and bottom waters of the shelf area throughout much of the Younger

Dryas (Eiríksson et al., 2000; Knudsen et al., 2004), and changes in the strength of the Irminger Current resulted in fluctuations in the sea-ice cover on the North Icelandic shelf. The increased influence of the Irminger Current caused an early melting of the base of the sea ice, but the ice edge/seasonal sea-ice cover prevailed at the surface between the generally permanent sea-ice conditions.

Interestingly, there was a distinct and rapid decrease in all biomarker concentrations at ca. 12.1 ka (Fig. 3), when the Vedde Ash was deposited. The Vedde tephra formed a peak in both the sand fraction and the mean grain size, as well as in the IRD in neighboring core HM107-05 (Eiríksson et al., 2000; Knudsen et al., 2004). This would explain the decreased and low biomarker concentrations, as the accumulation of organic materials is nor-

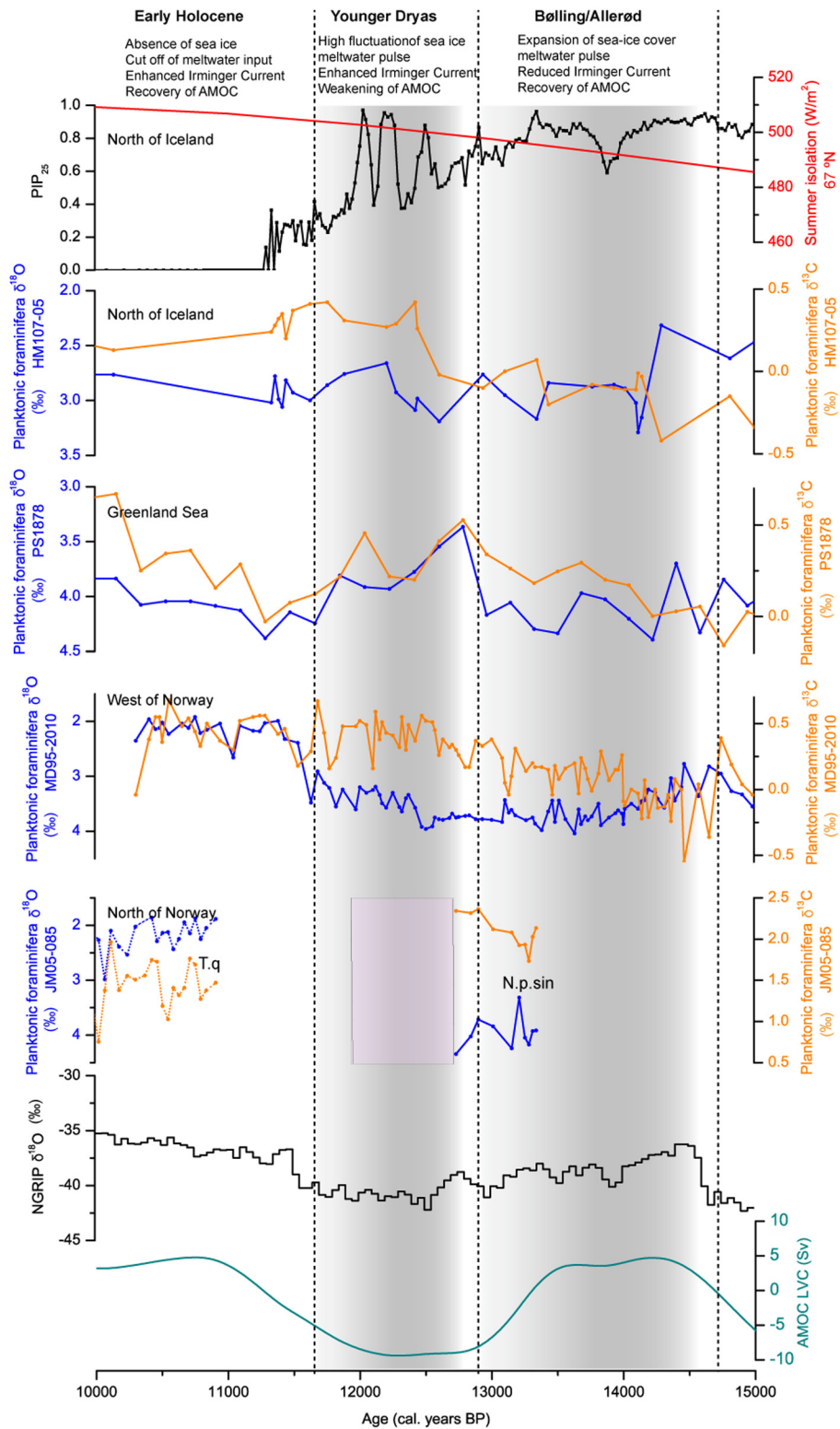


Fig. 5. Compilation of Nordic Seas proxies and model data documenting atmospheric and oceanic changes during the last deglaciation. Insolation displays changes in the atmosphere (<http://vo.imcce.fr/insola/earth/online/earth/online/>). AMOC changes were simulated by modeling (Ritz et al., 2013). NGRIP $\delta^{18}\text{O}$ data were obtained from the Greenland ice core (Rasmussen et al., 2006). The isotope data from core HM107-05 (Eiriksson et al., 2000; Knudsen et al., 2004); PS1878 (Telesinski et al., 2014b); MD95-2010 (Dokken and Jansen, 1999); JM05-085 (Aagaard-Sorensen et al., 2010). The pink bar indicates an interval barren of the planktonic foraminifera. T.q = *Turborotalita quinqueloba*; N.p. sin = *Neoglobobadrina pachyderma* sinistral. (For interpretation of the references to color in this figure legend, the reader is referred to the web version of this article.)

mally low in coarse sediments. Also, the Vedde tephra horizon of core HM107-05 was totally barren of foraminifera (Eiriksson et al., 2000; Knudsen et al., 2004). The maximum values of both IP₂₅ and *n*-alkanols before and after the Vedde Ash of MD99-2272

reflect a freshwater peak triggering the sea-ice formation at the core site (Fig. 3). This is consistent with a decrease in $\delta^{18}\text{O}$ values just below the Vedde tephra horizon, continuing to the end of the Younger Dryas in core HM107-05. This indicates that the interval

presumably represented a sea surface freshwater peak, combined with brine formation (Knudsen et al., 2004). A Younger Dryas melt-water spike has also been observed before the Vedde Ash Zone in the Greenland Sea (Fig. 5; Telesinski et al., 2014a, 2014b), suggesting that a freshwater discharge could be considered as a trigger for the Younger Dryas.

Furthermore, the summer insolation during the Younger Dryas became higher than that during the Bølling/Allerød (Figs. 4 and 5). The influence of the Irminger Current (Eiriksson et al., 2000; Knudsen et al., 2004) and the increased insolation resulted in a reduction of sea-ice coverage towards the end of the Younger Dryas (Fig. 3). This agrees well with the change from abundant sea-ice diatom species to warm water species on the North Iceland Shelf towards the end of the Younger Dryas (Knudsen et al., 2004).

IP₂₅ and PIP₂₅ records from the Yermak Plateau and west of Svalbard (Fig. 1) indicated an almost perennial sea-ice coverage at the early stage of the Younger Dryas and less sea-ice coverage during the Mid- and Late Younger Dryas when the warm Atlantic Water could penetrate to the Arctic through the Fram Strait (Müller et al., 2009; Müller and Stein, 2014). In the western Barents Sea and northwest of Norway in the eastern Nordic Seas (Fig. 1), extensive and seasonal sea-ice conditions were revealed by IP₂₅ and PIP₂₅ records, respectively (Cabedo-Sanz et al., 2013; Belt et al., 2015). Thus, IP₂₅ and PIP₂₅ in sediment cores from both the northern Nordic Seas (Fram Strait) and the eastern Nordic Seas (Fig. 1) displayed obvious peak values during the cold Younger Dryas interval compared to the previous Bølling/Allerød and the subsequent Holocene period (Figs. 4 and A3), in contrast to fluctuating sea-ice conditions on the North Icelandic shelf.

5.3. Climatic amelioration from the Early to Mid-Holocene (11.7–4.0 ka)

At the onset of the Holocene (ca. 11.7–11.3 ka), IP₂₅ dropped to zero values while brassicasterol concentrations were high (Fig. 3). The P_BIP₂₅ index decreased from around 0.4 to 0, indicating continuous retreat of the spring sea-ice extent, with occurrences of shorter periods of seasonal sea ice. The total absence of IP₂₅ and the persistent high brassicasterol concentrations during part of the Early and Mid-Holocene (ca. 11.3–6.8 ka) most likely indicate ice-free conditions throughout the year on the North Icelandic shelf (Fig. 3; cf. Müller et al., 2011), consistent with an abrupt increase in NGRIP $\delta^{18}\text{O}$ (Fig. 5). However, a minor contribution from the winter sea ice cannot be excluded as IP₂₅ is an indicator of spring sea ice (Müller et al., 2011). Significantly, HBI triene concentration increased to its highest values during this time interval (Fig. A1). This was caused by the Early Holocene warming as reflected by zero PIP₂₅ values (Figs. 3 and A1). The diatom and foraminiferal assemblages were composed mainly of warm species, and the cold-water and sea-ice species decreased to low frequencies (Knudsen et al., 2004), reflecting that the North Icelandic shelf was dominated by the Irminger Current. The maximum insolation and enhanced warm Atlantic Water inflow stimulated the productivity of phytoplankton and restricted sea-ice formation (Figs. 4 and 5).

IP₂₅ is detectable at low concentration during the Mid-Holocene from ca. 6.8 to 4 ka (Fig. 3). This coincides with an increase in the percentage of the polar planktonic foraminifera *Neogloboquadrina pachyderma* (sinistral) to more than 95% in the neighboring core HM107-05 with a similar oceanographic setting as MD99-2272. Together, these results indicate an increase in the influence of Arctic or Polar water masses on the North Icelandic shelf (Knudsen et al., 2004). A generally increased IRD from ice-bbergs or sea ice along the North Icelandic shelf also indicated a general cooling of the surface water at this site (Eiriksson et al., 2000; Knudsen et al., 2004). Brassicasterol concentrations were also elevated after ca. 7 ka at MD99-2272. This is consistent with the increased biogenic carbonate in the nearby core MD99-2269 and the highest pro-

ductivity of phytoplanktonic and benthic foraminifera on the East Greenland Shelf during the Mid-Holocene (Giraudeau et al., 2004; Cabedo-Sanz et al., 2016).

During the Early to Mid-Holocene, the North Icelandic shelf was characterized by reduced sea-ice cover indicating climate amelioration. Similarly, ice-free/less sea-ice conditions during the Early Holocene are indicated by the IP₂₅/PIP₂₅ records of sediment cores from the Fram Strait and the eastern Nordic Seas (Fig. 4). Additionally, an increase in sea ice after 6.8 ka during the Mid-Holocene on the North Icelandic shelf is consistent with a general cooling and an increased sea-ice scenario in Fram Strait and Eastern Greenland shelf, also based on IP₂₅ study (Müller et al., 2012). Therefore, the Holocene sea-ice conditions in the western Nordic Seas and neighboring regions generally showed in-phase changes.

5.4. Implications for regional oceanic variability

Our biomarker data constitute the first record of rapid sea-ice variability on the North Icelandic shelf through the transition from the last deglaciation to the Holocene, reflecting the unstable and complex climate situation in the region. A synthesis of our data and previously published data affords a more detailed discussion on the link between the recurrent advance and retreat of sea ice during the last deglaciation (15–11.7 ka) with significant variability in ocean circulation in the Nordic Seas.

The Bølling/Allerød interval was generally warm as recorded in the Greenland NGRIP ice core (Fig. 5). However, the North Icelandic shelf was characterized by an extensive sea-ice cover indicated by our biomarker data, probably caused by ocean circulation changes (Fig. 6a). This region was dominated by the enhanced East Greenland Current and East Icelandic Current, while the Irminger Current was reduced and the marine sediments contained basaltic pebbles from ice-bbergs or drift-ice floes, reflecting the cooling of the surface water on the North Icelandic shelf (Eiriksson et al., 2000). Modeling results show that an enhanced Norwegian Current leads to the weakening of the Irminger Current to the Icelandic shelf, and, inversely, a reduction of the Norwegian Current leads to warming of the Iceland Sea (Drange et al., 2005). Giraudeau et al. (2004) also suggested that the strength of Atlantic inflow into the Nordic Seas was subjected to a balance between the Irminger and the Norwegian branches. Isotope records from the Greenland Sea and west of Norway (Figs. 1 and 5) also indicate that increased influence of the East Greenland Current in the western Nordic Seas coincides with enhanced Atlantic Water inflow to the eastern Nordic Seas (Dokken and Jansen, 1999; Telesinski et al., 2014b). A strengthening of North Atlantic Water inflow to the eastern Nordic Seas led to deep-water formation, and thus a recovery of the AMOC (Fig. 5; Ritz et al., 2013). Therefore, a cooling of surface waters north of Iceland, characterized by the extensive spring and summer sea-ice cover and pronounced cold bottom water, was probably related to the onset of Nordic Seas deep-water formation and recovery of AMOC. Since the Iceland, Greenland and Svalbard ice sheets retreated from the shelves to the fjords and the cold freshwater prevailed in the central Nordic Sea during the Bølling/Allerød, sea ice prevailed throughout the spring and summer in the Nordic Seas except the marginal areas of the eastern Nordic Seas which were influenced by the penetration of warm, saline Atlantic Water (Knudsen et al., 2004; Ślubowska-Woldengen et al., 2008). The Icelandic shelf and the eastern margin of the Nordic Seas thus displayed an obvious seesaw pattern in the flow of the Atlantic Water and in sea-ice distribution (Fig. 6a).

The Younger Dryas cold period has been commonly considered as driven by freshwater forcing on the ocean surface that hampered NADW formation and thereby reduced the northward heat advection of Atlantic Water. The East Icelandic Current was

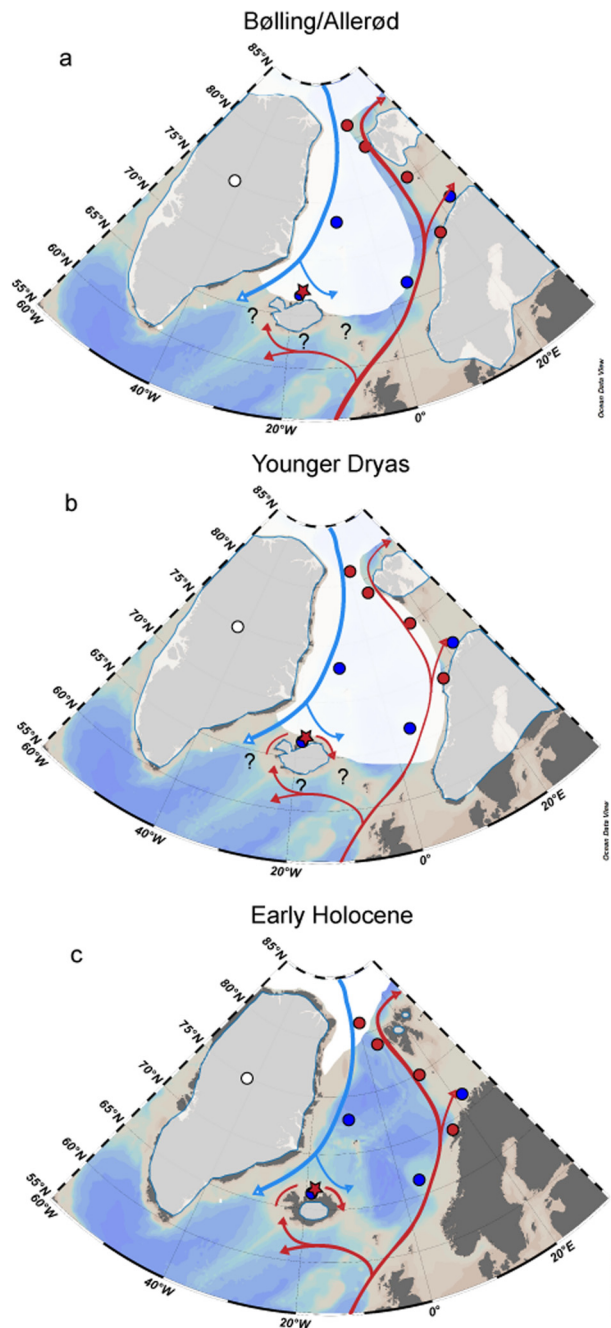


Fig. 6. Schematic illustration of last deglaciation to Holocene changes of spring/summer sea-ice conditions (white shadings) for the study areas as reconstructed from biomarker data. Extent of continental ice sheets (transparent shadings with blue edge) during the Bølling/Allerød after Ślubowska-Woldengen et al. (2008) and during the Younger Dryas after Bradley and England (2008). Red arrows refer to the Atlantic Water advection, and blue arrows show the cold Polar water from the Arctic Ocean. For explanation of the dots, see Fig. 1. (For interpretation of the references to color in this figure legend, the reader is referred to the web version of this article.)

dominant on the North Icelandic shelf but a periodic flux of an enhanced Irminger Current also occurred (Eiriksson et al., 2000). During the Younger Dryas interval, the increased deposition of the IRD in marine sediments from the Nordic Seas indicates fluctuation and re-advance of glacier and/or sea ice in fjords and on shelves of Scandinavia and Iceland (Eiriksson et al., 2000; Bauch et al., 2001; Knudsen et al., 2004). The shelf bottom waters along the margin of the eastern Nordic Seas were cold with low salinity. In contrast, chilled Atlantic subsurface water flowed to the North Icelandic shelf below the cold and fresh surface water (stratified water col-

umn). A less pronounced meltwater event with brine formation occurred during the Younger Dryas, with the Vedde Ash deposited within this interval. During the Younger Dryas, there was no significant cooling accompanied by the influence of the Irminger Current in subsurface waters of the North Icelandic shelf (Knudsen et al., 2004). The Younger Dryas was thus characterized by a continuous strong East Iceland Current, a fluctuating influx of the Irminger Current and sea-ice cover on the North Icelandic shelf (Fig. 6a). Heavy $\delta^{18}\text{O}$ values in a sediment core from the west of Norway and lack of planktonic foraminifera in a sediment core from off northern Norway during the Younger Dryas (Figs. 1 and 5) indicate a cold scenario in the eastern Nordic Seas (Dokken and Jansen, 1999; Aagaard-Sørensen et al., 2010). Compared to the cooling event in the Nordic Seas region (e.g. Greenland, Northern Europe and the eastern Nordic Seas), the warming of the North Icelandic shelf bottom waters indicated a northward displacement of the Polar Front in the western North Atlantic. The strengthening of the Irminger Current may have been caused by the western deflection of the North Atlantic Current (Eiriksson et al., 2000), resulting in less severe sea-ice conditions than those during the Bølling/Allerød interval (Fig. 6a and b).

The Late-glacial anti-phase relationship in the oceanic environment between the North Icelandic shelf and the eastern Nordic Seas switched to an in-phase situation when entering the Holocene. The IRD content is low in sediments from the entire Nordic Sea during the Early Holocene (Eiriksson et al., 2000; Klitgaard-Kristensen et al., 2001; Knudsen et al., 2004; Ślubowska-Woldengen et al., 2008), indicating an absence of sea ice in the area (Fig. 6c). Bauch et al. (2001) also reported that the freshwater input to the central Nordic Sea from melting ice-bergs was completely cut off at around 10.0 ka. The decrease of sea ice and climatic amelioration on the North Icelandic shelf were caused by the enhanced influence of the warm Irminger Current and maximum insolation. There was also a pronounced warming in the eastern North Atlantic (cf. Klitgaard-Kristensen et al., 2001) with warm Atlantic Water penetrating to the northern Norwegian shelf and increased deep-water formation. In addition, the recovery of the AMOC after 11.7 ka (Fig. 5; Ritz et al., 2013) further supported a significant heat transport from the tropical area to the Nordic Seas (McManus et al., 2004).

6. Conclusion

For the first time, North Icelandic shelf sea-ice variability throughout the Late-glacial and Early to Mid-Holocene is reconstructed from biomarker data in a marine sediment core. A comparison with records from Nordic Seas sediment cores, the Greenland NGRIP ice core and modeling data is presented. Sea-ice variability on the North Icelandic shelf is linked to broader regional changes in the northern North Atlantic. The results show a Late-glacial oceanic seesaw pattern between the western and eastern Nordic Seas, while an in-phase relationship prevailed during the Holocene. The sea-ice variability and warm/cold oscillations in the area were related to the variability of deep-water formation and AMOC. The main conclusions for the North Icelandic sea-ice history during the Late-glacial and Early to Mid-Holocene and its relationship to the oceanic environment are:

1. Spring sea ice extended across the core site on the North Icelandic shelf during the Bølling/Allerød (14.7–12.9 ka), caused by a reduction of Irminger Current and increase of the East Iceland Current, as well as a meltwater pulse. This is in contrast to ice-free conditions in the margins of the eastern Nordic Seas with enhanced Norwegian Current inflow.

2. Spring sea ice still prevailed on the North Icelandic shelf during the Younger Dryas interval (12.9–11.7 ka), but seasonal sea ice occurred occasionally and was less severe than during the

Bølling/Allerød. This was related to a short interval of enhanced Irminger Current on the North Icelandic shelf and is in contrast to increased sea–ice cover in the eastern Nordic Seas caused by a reduction of the inflow of the Atlantic Water inflow to that area.

3. Sea ice was totally absent during the Early Holocene and part of the Mid-Holocene interval (11.7–6.8 ka), when insolation reached its maximum after the deglaciation; but a re-advance of sea ice occurred during the Mid-Holocene (6.8–4 ka). These results from the North Icelandic shelf are consistent with the sea–ice variability in the eastern Nordic Seas.

Acknowledgements

We acknowledge the facilities provided by the Institut Paul-Emil Victor (IPEV) for IMAGES coring operation onboard the R/V Marion Dufresne in 1999. We are grateful to Hailong Zhang for technical support. We also thank three anonymous reviewers for numerous helpful comments for improving the manuscript. This work was supported by the National Natural Science Foundation of China (Grant Nos. 41506214, 41520104009, 41521064 and 41406209); China Postdoctoral Science Foundation (Grant No. 2015M572081); and by “111” project (B13030). This is MCTL contribution #126.

Appendix. Supplementary material

Supplementary material related to this article can be found online at <http://dx.doi.org/10.1016/j.epsl.2017.05.006>.

References

- Aagaard-Sørensen, S., Husum, K., Hald, M., Knies, J., 2010. Paleoceanographic development in the SW Barents Sea during the Late Weichselian Early Holocene transition. *Quat. Sci. Rev.* 29, 3442–3456.
- Andrews, J.T., Belt, S.T., Olafsdóttir, S., Massé, G., Vare, L.L., 2009. Sea ice and marine climate variability for NW Iceland/Denmark Strait over the last 2000 cal. yr BP. *Holocene* 19, 775–784.
- Axford, Y., Andresen, C.S., Andrews, J.T., Belt, S.T., Geirsdóttir, Á., Massé, G., Miller, G.H., Ólafsdóttir, S., Vare, L.L., 2011. Do paleoclimate proxies agree? A test comparing 19 late Holocene climate and sea–ice reconstructions from Icelandic marine and lake sediments. *J. Quat. Sci.* 26, 645–656.
- Bakke, J., Lie, O., Heegaard, E., Dokken, T., Haug, G.H., Birks, H.H., Dulski, P., Nilsen, T., 2009. Rapid oceanic and atmospheric changes during the Younger Dryas cold period. *Nat. Geosci.* 2 (3), 202–205.
- Bauch, H.A., Erlenkeuser, H., Spielhagen, R.F., Struck, U., Matthiessen, J., Thiede, J., Heinemeier, J., 2001. A multiproxy reconstruction of the evolution of deep and surface waters in the subarctic Nordic Seas over the last 30,000 yr. *Quat. Sci. Rev.* 20, 659–678.
- Belt, S.T., Massé, G., Rowland, S.J., Poulin, M., Michel, C., LeBlanc, B., 2007. A novel chemical fossil of palaeo sea ice: IP₂₅. *Org. Geochem.* 38 (1), 16–27.
- Belt, S.T., Müller, J., 2013. The Arctic sea ice biomarker IP₂₅: a review of current understanding, recommendations for future research and applications in palaeo sea ice reconstructions. *Quat. Sci. Rev.* 79 (1), 9–25.
- Belt, S.T., Cabedo-Sanz, P., Smik, L., Navarro-Rodriguez, A., Berben, S.M.P., Knies, J., Husum, K., 2015. Identification of paleo Arctic winter sea ice limits and the marginal ice zone: optimised biomarker-based reconstructions of late Quaternary Arctic sea ice. *Earth Planet. Sci. Lett.* 431, 127–139.
- Brown, T.A., Belt, S.T., Tatarek, A., Mundy, C.J., 2014. Source identification of the Arctic sea ice proxy IP₂₅. *Nat. Commun.* 5, 4197.
- Cabedo-Sanz, P., Belt, S.T., Knies, J., Husum, K., 2013. Identification of contrasting seasonal sea ice conditions during the Younger Dryas. *Quat. Sci. Rev.* 79, 74–86.
- Cabedo-Sanz, P., Belt, S.T., Jennings, A.E., Andrews, J.T., Geirsdóttir, Á., 2016. Variability in drift ice export from the Arctic Ocean to the North Icelandic Shelf over the last 8000 years: a multi-proxy evaluation. *Quat. Sci. Rev.* 146, 99–115.
- Dokken, T.M., Jansen, E., 1999. Rapid changes in the mechanism of ocean convection during the last glacial period. *Nature* 401, 458–461.
- Drange, H., Dokken, T., Furevik, T., Gerdes, R., Berger, W., 2005. The Nordic Seas: An Integrated Perspective Oceanography, Climatology, Biogeochemistry, and Modelling. *Geophys. Monogr.*, vol. 158. American Geophysical Union, 366 pp.
- Eiriksson, J., Knudsen, K.L., Hafliðason, H., Henriksen, P., 2000. Late-glacial and Holocene paleoceanography of the North Icelandic shelf. *J. Quat. Sci.* 15 (1), 23–42.
- Englinton, T.I., Englinton, G., 2008. Molecular proxies for paleoclimatology. *Earth Planet. Sci. Lett.* 275, 1–16.
- Giraudeau, J., Jennings, A., Andrews, J., 2004. Timing and mechanisms of surface and intermediate water circulation changes in the Nordic Seas over the last 10,000 cal.years: a view from the North Icelandic shelf. *Quat. Sci. Rev.* 23, 2127–2139.
- Gudmundsdóttir, E.R., Larsen, G., Eiriksson, J., 2012. Tephra stratigraphy on the North Icelandic shelf: extending tephrochronology into marine sediments off North Iceland. *Boreas* 41 (4), 719–734.
- Hubbard, A., Sugden, D., Dugmore, A., Norddahl, H., Pétursson, H.G., 2006. A modelling insight into the Icelandic Last Glacial Maximum ice sheet. *Quat. Sci. Rev.* 25 (17–18), 2283–2296.
- Ingólfsson, Ó., Benediktsson, Í.Ö., Schomacker, A., Kjær, K.H., Brynjólfsson, S., Jónsson, S.A., Korsgaard, N.J., Johnson, M.D., 2016. Glacial geological studies of surge-type glaciers in Iceland – research status and future challenges. *Earth-Sci. Rev.* 152, 37–69.
- Jiang, H., Muscheler, R., Björck, S., Seidenkrantz, M., Olsen, J., Sha, L., Sjolte, J., Eiriksson, J., Ran, L., Knudsen, K.L., Knudsen, M.F., 2015. Solar forcing of Holocene summer sea-surface temperatures in the northern North Atlantic. *Geology* 43 (3), 203–206.
- Klitgaard-Kristensen, D., Sejrup, H.P., Hafliðason, H., 2001. The last 18 kyr fluctuations in Norwegian Sea surface conditions and implications for the magnitude of climatic change: evidence from the North Sea. *Paleoceanography* 16 (5), 455–467.
- Knies, J., 2005. Climate-induced changes in sedimentary regimes for organic matter supply on the continental shelf off northern Norway. *Geochim. Cosmochim. Acta* 69, 4631–4647.
- Knudsen, K.L., Eiriksson, J., 2002. Application of tephrochronology to the timing and correlation of palaeoceanographic events recorded in Holocene and Lateglacial shelf sediments off North Iceland. *Mar. Geol.* 191, 165–188.
- Knudsen, K.L., Jiang, H., Jansen, E., Eiriksson, J., Heinemeier, J., Seidenkrantz, M.S., 2004. Environmental changes off North Iceland during the deglaciation and the Holocene: foraminifera, diatoms and stable isotopes. *Mar. Micropaleontol.* 50, 273–305.
- Larsen, G., Eiriksson, J., Knudsen, K.L., Heinemeier, J., 2002. Correlation of late Holocene terrestrial and marine tephra markers in North Iceland. Implications for reservoir age changes and linking land–sea chronologies in the northern North Atlantic. *Polar Res.* 21, 283–290.
- Massé, G., Rowland, S.J., Sicre, M.-A., Jacob, J., Jansen, E., Belt, S.T., 2008. Abrupt climate changes for Iceland during the last millennium: evidence from high resolution sea ice reconstructions. *Earth Planet. Sci. Lett.* 269, 565–569.
- McManus, J.F., Francois, R., Gherardi, J.M., Keigwin, L.D., Brown-Leger, S., 2004. Collapse and rapid resumption of Atlantic meridional circulation linked to deglacial climate changes. *Nature* 428 (6985), 834–837.
- Müller, J., Massé, G., Stein, R., Belt, S.T., 2009. Variability of sea–ice conditions in the Fram Strait over the past 30,000 years. *Nat. Geosci.* 2 (11), 772–776.
- Müller, J., Wagner, A., Fahl, K., Stein, R., Prange, M., Lohmann, G., 2011. Towards quantitative sea ice reconstructions in the northern North Atlantic: a combined biomarker and numerical modelling approach. *Earth Planet. Sci. Lett.* 306, 137–148.
- Müller, J., Werner, K., Stein, R., Fahl, K., Moros, M., Jansen, E., 2012. Holocene cooling culminates in sea ice oscillations in Fram Strait. *Quat. Sci. Rev.* 47, 1–14.
- Müller, J., Stein, R., 2014. High-resolution reconstruction of sea ice conditions in Fram Strait sheds new light on late glacial and deglacial climate variability. *Earth Planet. Sci. Lett.* 403, 446–455.
- Not, C., Hillaire-Marcel, C., 2012. Enhanced sea–ice export from the Arctic during the Younger Dryas. *Nat. Commun.* 3, 647.
- Norðdahl, H., Ingólfsson, Ó., 2015. Collapse of the Icelandic ice sheet controlled by sea-level rise? *Arktos* 1, 1–13.
- Rasmussen, S.O., Andersen, K.K., Svensson, A.M., Steffensen, J.P., Vinther, B.M., Clausen, H.B., Siggaard-Andersen, M.-L., Johnsen, S.J., Larsen, L.B., Dahl-Jensen, D., Bigler, M., Röthlisberger, R., Fischer, H., Goto-Azuma, K., Hansson, M.E., Ruth, U., 2006. A new Greenland ice core chronology for the last glacial termination. *J. Geophys. Res.* 111, D06102.
- Rayner, D., Hirschi, J.J.M., Kanzow, T., Johns, W.E., Wright, P.G., Frajka-Williams, E., Bryden, H.L., Meinen, C.S., Baringer, M.O., Marotzke, J., Beal, L.M., Cunningham, S.A., 2011. Monitoring the Atlantic meridional overturning circulation. *Deep-Sea Res.* 58, 1744–1753.
- Ritz, S.P., Stocker, T.F., Grimalt, J.O., Menviel, L., Timmermann, A., 2013. Estimated strength of the Atlantic overturning circulation during the last deglaciation. *Nat. Geosci.* 6 (3), 208–212.
- Rudels, B., Björck, G., Nilsson, J., Winsor, P., Lake, I., Nohr, C., 2005. The interaction between waters from the Arctic Ocean and the Nordic Seas north of Fram Strait and along the East Greenland Current: results from the Arctic Ocean-02 Oden expedition. *J. Mar. Syst.* 55 (1–2), 1–30.
- Schlitzer, R., 2017. *Ocean Data View*. <http://odv.awi.de/>.
- Schlüter, M., Sauter, E., 2000. Biogenic silica cycle in surface sediments of the Greenland Sea. *J. Mar. Syst.* 23 (4), 333–342.
- Smik, L., Cabedo-Sanz, P., Belt, S.T., 2016. Semi-quantitative estimates of paleo Arctic sea ice concentration based on source-specific highly branched isoprenoid alkenes: A further development of the PIP₂₅ index. *Org. Geochem.* 92, 63–69.
- Stein, R., Fahl, K., Müller, J., 2012. Proxy reconstruction of Arctic Ocean sea ice history: from IRD to IP₂₅. *Polarforschung* 82, 37–71.

- Stein, R., Fahl, K., Schreck, M., Knorr, G., Niessen, F., Forwick, M., Gebhardt, C., Jensen, L., Kaminski, M., Kopf, A., Matthiessen, J., Jokat, W., Lohmann, G., 2016. Evidence for ice-free summers in the late Miocene central Arctic Ocean. *Nat. Commun.* 7, 11148.
- Ślubowska-Woldengen, M., Koç, N., Rasmussen, T.L., Klitgaard-Kristensen, D., Hald, M., Jennings, A.E., 2008. Time-slice reconstructions of ocean circulation changes on the continental shelf in the Nordic and Barents Seas during the last 16,000 cal. yr B.P. *Quat. Sci. Rev.* 27, 1476–1492.
- Thornalley, D.J.R., Mccave, I.N., Elderfield, H., 2010. Freshwater input and abrupt deglacial climate change in the North Atlantic. *Paleoceanography* 25 (1), 83–104.
- Telesinski, M.M., Spielhagen, R.F., Lind, E.M., 2014a. A high-resolution Lateglacial and Holocene palaeoceanographic record from the Greenland Sea. *Boreas* 43, 273–285.
- Telesinski, M.M., Spielhagen, R.F., Bauch, H.A., 2014b. Water mass evolution of the Greenland Sea since late glacial times. *Clim. Past* 10, 123–136.
- Volkman, J.K., 2003. Sterols in microorganisms. *Appl. Microbiol. Biotechnol.* 60, 495–506.
- Xiao, X., Fahl, K., Müller, J., Stein, R., 2015. Sea-ice distribution in the modern Arctic Ocean: biomarker records from trans-Arctic Ocean surface sediments. *Geochim. Cosmochim. Acta* 155, 16–29.
- Zamelczyk, K., Rasmussen, T.L., Husum, K., Godtliebsen, F., Hald, M., 2014. Surface water conditions and calcium carbonate preservation in the Fram Strait during marine isotope stage (MIS) 2, 28.8–15.4 kyr. *Paleoceanography* 29 (1), 1–12.
- Zhao, M., Mercer, J.L., Eglinton, G., Teece, M., 2006. Comparative molecular biomarker assessment of phytoplankton paleoproductivity for the last 160 kyr off Cap Blanc, NW Africa. *Org. Geochem.* 37, 72–97.